

Constraining true polar wander and impactor source regions from modeling of elliptical crater orientations

For submission to ROSES –Solar System Workings 2017 (NNH17ZDA001N-SSW)

1. Table of contents.	0
2. Scientific/Technical/Management.	1
2.1 Summary.	1
2.2 Goals of the Proposed Study.	3
2.3 Scientific Background.	3
2.3.1 <i>The problem:</i> TPW and bombarder orbits are key unknowns for planetary history, but existing methods for their assessment would benefit from an independent constraint.	3
2.3.2. <i>Proposed solution:</i> Elliptical crater orientations record TPW and bombarder orbits.	4
2.3.3. <i>Preliminary work:</i> We have validated the data, built a flexible code base, and already retrieved a key geologic parameter using the method.	6
2.4 Technical Approach and Methodology.	9
2.4.1. Description of model	9
2.4.2. Task 1. Determine Mars TPW for the Amazonian and late Hesperian	10
2.4.3. Task 2. Constrain Mars TPW for the Noachian to Early Hesperian.....	11
2.4.4. Task 3. Constrain Mars bombarder orbits.	12
2.4.5. Assumptions and limitations.....	13
2.5 Perceived Impact of Proposed Work.	14
2.6 Work Plan.	15
2.7 Personnel and Qualifications.	15
3. References.	16
4. Data Management Plan.	21
5. Biographical sketches.	23
6. Summary Table of Work Effort.	25
7. Current and Pending Support.	26
8. Budget Justification.	28
8.1. Budget Narrative.	28
8.2. Facilities and Equipment.	28
8.3. Detailed budget, itemizing expenses.	28

2. Scientific/Technical/Management:

2.1 Summary. An asteroid or comet that strikes a planet $\lesssim 15^\circ$ from the horizon leaves an elongate scar. These scars – **elliptical impact craters** – **retain a record of the arrival direction of impactors, via their long-axis orientations** (Fig. 1). The orientations of elliptical craters on Mars are anisotropic, with an overall $>10\sigma$ excess of N-S oriented craters (Fig. 2). These anisotropies are not the result of post-impact modification, nor systematic nor random measurement errors, nor projection effects, but are a probe of the impact geometry (§2.3.2). Impact geometry for any given impact is stochastic, because the exact trajectory (and associated gravity focusing) of each incoming bolide is subject to randomness. However, this random behavior can be marginalized over, because $>10^4$ elliptical crater orientations are publicly available for a target world of interest, Mars (Robbins & Hynes 2012). Given a target world’s orbital parameters, **the resulting, appropriately-marginalized impact geometries are set by the orientation of the target world’s lithosphere in inertial space (obliquity plus true polar wander), and the orbital elements of the impactors (Fig. 1).**

In our preliminary study (§2.3.3; Holo, Kite, and Robbins, in review), we used crater-orientation data to retrieve the Late Hesperian and Amazonian obliquity history of Mars. As shown in our preliminary work (§2.3, §2.4), it is straightforward to unscramble the contributions of these three factors, because **each has unique effects on the distribution of elliptical crater orientations (Fig. 1)**. Each of these three factors – obliquity, true polar wander (TPW), and the orbital elements of the impactors – is of critical importance for solar system history. Specifically, for Mars, obliquity is important for Mars climate (e.g., Toon 1980, Jakosky & Carr 1985, Jakosky et al. 1995, Forget et al. 2006, Wordsworth 2016), true polar wander is important for Mars tectonics and paleoclimate (Bouley et al. 2016, Perron et al. 2007), and the orbital elements of the impactors that struck Mars are important for understanding the source of the “Late Heavy Bombardment” (e.g. Bottke & Norman 2017, and references therein). **We propose to refine, develop and apply models to fully exploit the elliptical-crater orientation proxy for Mars in order to constrain net true polar wander, and the orbital elements of bombarding populations, during the Noachian and Early Hesperian periods.** The proposed work builds on a completed project on the Amazonian and Late Hesperian period of Mars history (§2.3.3). We select Mars because a $>10^4$ -crater database of elliptic craters already exists for Mars (Fig. 2), and because Mars’ history of TPW and bombardment is interesting and controversial (§2.3.1; Fig. 3; Melosh 1980). Specifically (Fig. 1), we will first seek the longitudinal twist that TPW imparts to long-axis orientations in our existing Late Hesperian and Amazonian dataset. We anticipate that this will set a new and tight constraint on post-3.2 Ga net TPW. Next, we will marginalize over the (unknown) Noachian and early Hesperian obliquity in order to retrieve Noachian and early Hesperian TPW. In parallel, we will use the amplitude of the Noachian/Early Hesperian crater-anisotropy signal (Fig. 2) to constrain the source region of the LHB bombarders. In summary, we propose a basic and direct method that offers a new approach (complementary to existing methods) for retrieving Solar System history parameters that have been sought for more than three decades.

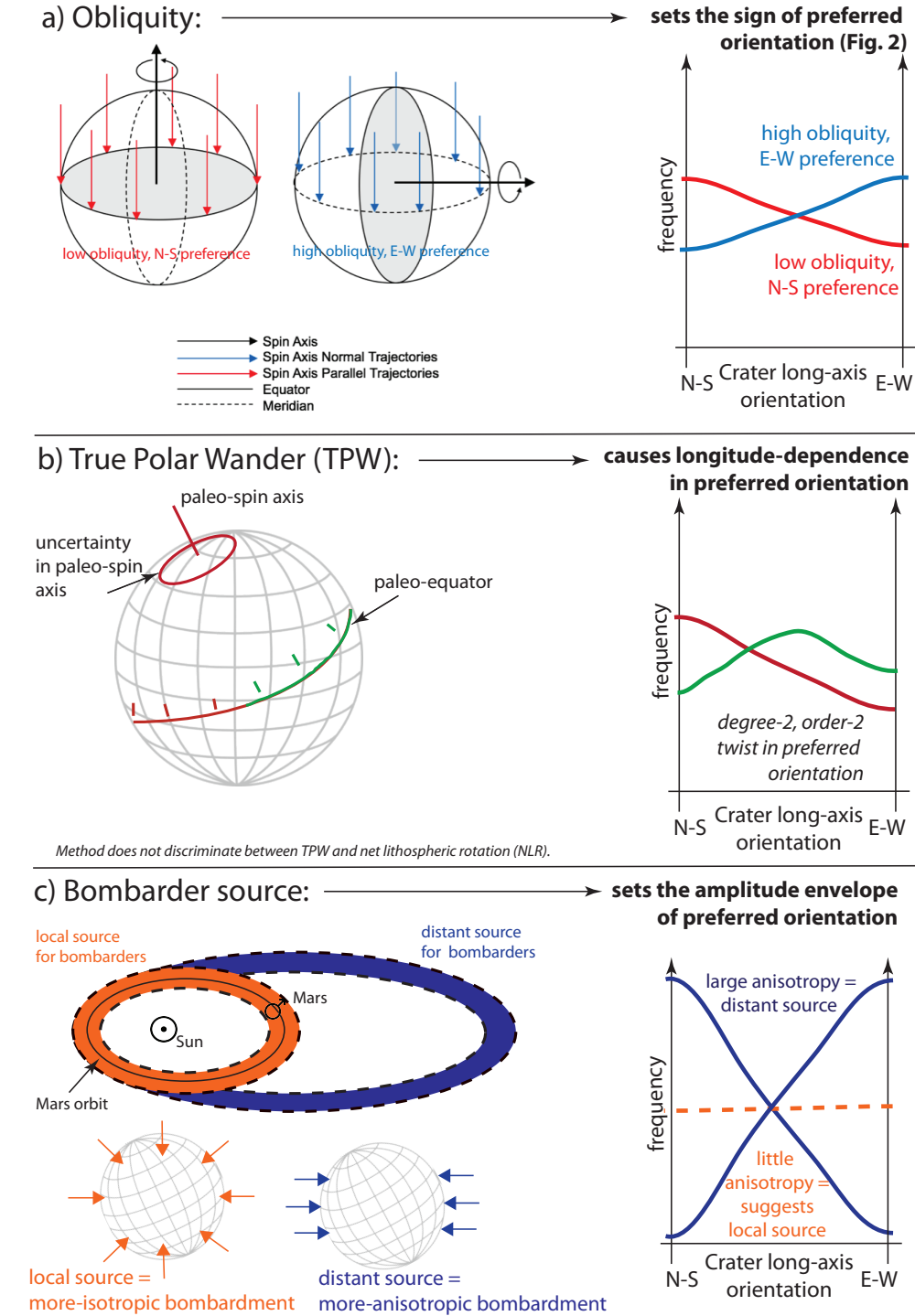


Fig. 1. Obliquity, TPW, and bombarder orbits cause distinct and distinguishable contributions to Mars elliptical-crater orientations (§2.3.3). Impactors approaching parallel to spin axis yield N-S elliptic craters near the equator, while impactors approaching normal to spin axis produce elliptic craters that are E-W oriented at all latitudes except near the pole. Other metrics, such as latitude-dependence, can also be used to further discriminate and cross-check the results. The effects of gravity focusing are included in our numerical model, but not shown here for simplicity.

2.2 Goal of the proposed study.

The goal of the proposed work is to constrain TPW and impactor source regions from modeling of elliptical craters. Achieving this goal involves the following objectives:-

- Modify our existing model for Mars, to determine net Mars TPW for the Late-Hesperian-Amazonian (§2.4.2).
- Constrain net Mars TPW for the Noachian to Early Hesperian (§2.4.3).
- Constrain Mars bombarder orbits for the Noachian to Early Hesperian (§2.4.4).

In order to define a focused, well-posed investigation of appropriate scope for a three-year study, we make several simplifying assumptions, which are explained and justified in §2.4.5.

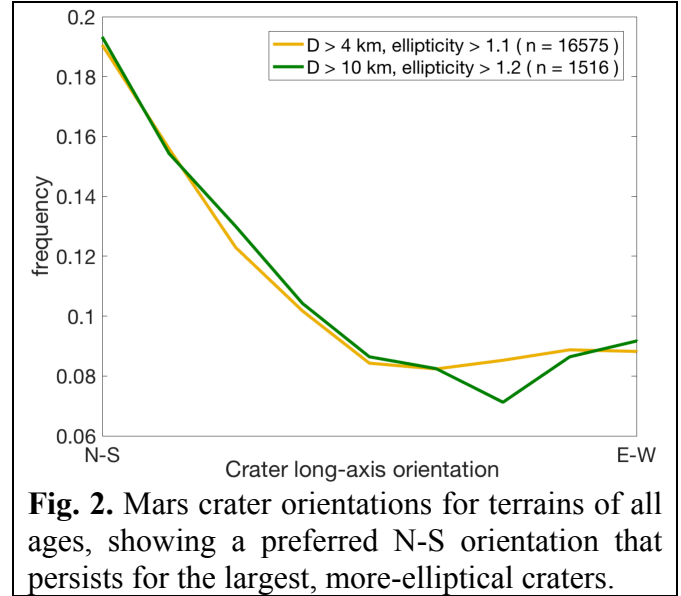


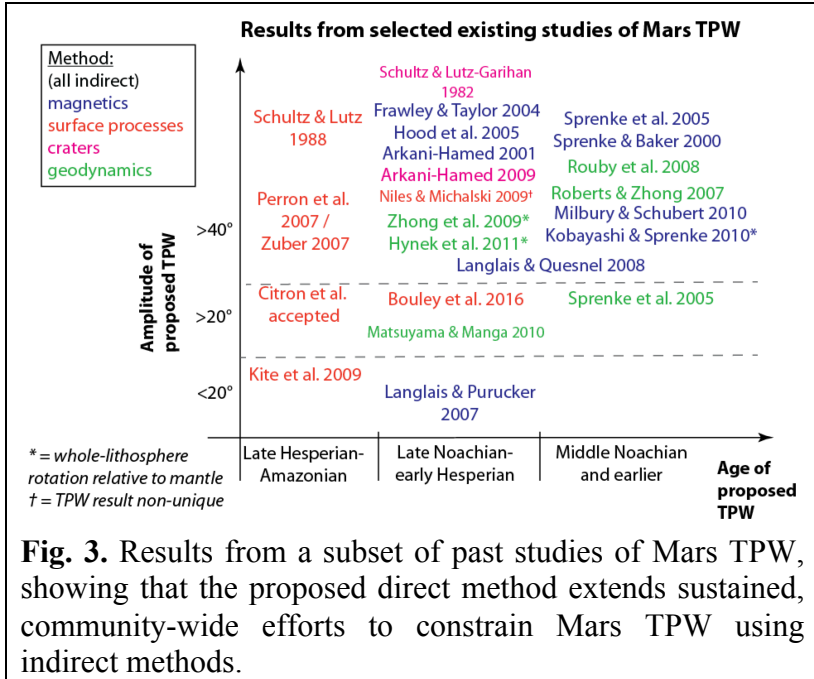
Fig. 2. Mars crater orientations for terrains of all ages, showing a preferred N-S orientation that persists for the largest, more-elliptical craters.

2.3 Scientific background.

2.3.1. *The problem:* TPW and bombarder orbits are key unknowns for planetary history, but existing methods for their assessment would benefit from an independent constraint.

True Polar Wander: On worlds that lack evidence for plate tectonics, such as Mars, the Moon, Pluto, and Enceladus, True Polar Wander is the main process of latitudinal reorientation (Gold 1955, Matsuyama 2014, Keane et al. 2016). Latitudinal reorientation is key for volatile stabilization/destabilization, fault/fracture formation and the locations of tidal heating, and for understanding the dynamics of internal mass anomalies, such as mantle plumes. In addition to these direct effects of TPW, the geographic shifts due to TPW are key for paleoclimate and dynamo reconstruction. The importance of TPW explains the high profile of recent studies reporting evidence for True Polar Wander beyond Earth (Nimmo & Pappalardo 2006, Perron et al. 2007, Schenk et al. 2008, Keane et al. 2016, Siegler et al. 2016, Bouley et al. 2016). However, in all off-Earth cases, the evidence for TPW lacks the certainty that can be achieved for Earth TPW (for which paleomagnetic analysis of oriented samples proves Phanerozoic TPW; e.g. Steinberger & Torsvik 2008). To the contrary, evidence for TPW beyond Earth is circumstantial and/or indirect. Because the evidence is circumstantial and/or indirect, alternative interpretations remain possible (e.g. Scanlon et al. 2018 vs. Kite et al. 2009). Indeed, the notion of large-amplitude TPW has been challenged (Grimm & Solomon 1986, Matsuyama and Manga 2010, Tsai and Stevenson 2007, Harada et al. 2012). Mars is the ideal world for a direct test of the controversial and important TPW idea. That is because the indirect evidence for TPW at Mars is considered to be relatively strong by specialists in rotational dynamics (Matsuyama et al. 2014), and comes from so many lines of evidence (Fig. 3) – although these lines of evidence do not always agree with one another (Fig. 3). Thus if a direct test rejects the TPW hypothesis at Mars, that would be surprising and interesting. We propose to carry out a direct test.

Bombarder orbits: *Where did the bolides that formed the oldest craters to have been preserved in the Solar System geologic record come from?* This question has vexed planetary scientists for over 40 years. That is because multiple interpretations are possible with existing methods (e.g. Fassett & Minton 2013, Morbidelli et al. 2015, Bottke & Norman 2017). Existing methods use geochemistry and N-body simulations. Although the geochemistry of impactors is independently interesting, and D/H data disfavor a periodic-comet-like isotopic composition



for the LHB impactors (e.g. Altwegg et al. 2015), 40 years of application of these methods has not led to convergence on the dynamical source. This is in part because mixing very early in Solar System history may scramble geochemical fingerprints (e.g. Brownlee 2014, Batygin & Laughlin 2015). Crater size-frequency distributions (e.g. R-plots) might constrain the processes that shaped the bombarder population (Strom et al. 2005; but see also Orgel et al. 2018), but again do not directly constrain their source region in the solar system. Yet the location of the source region (e.g. clean-up of the terrestrial planet region, vs. asteroid belt, vs. more distant source) is a key metric for accepting or rejecting N-body models of ancient bombardments. Currently, all 3 hypotheses are considered by dynamicists and geochemists to be actively in play (Bottke & Norman 2017). We propose a basic, direct method (Fig. 1) that offers a new approach for constraining these hypotheses, complementary to existing methods.

2.3.2. Proposed solution: Elliptical crater orientations record TPW and bombarder orbits.

The anisotropy in the flux of asteroids to inner-solar-system worlds is well known (e.g. Bottke et al. 2002), and is responsible (for example) for <30% deviations from impact flux uniformity with latitude on the terrestrial planets (Le Feuvre and Weiczorek 2008). We propose to exploit one attribute of this well-known anisotropy: specifically, the anisotropy in relative-velocity vectors. Most craters on Mars are near-circular, but impactors with small impact angles relative to the surface produce elliptic craters with major axes aligned with impactor velocity vector (the threshold angle is $\lesssim 15^\circ$ and velocity-dependent; Bottke et al. 2000b, Collins et al. 2011). As a result, impactors that travel parallel to Mars' spin pole will create North-South oriented craters at the equator, and impactors that travel normal to the spin pole will create elliptic craters at all latitudes that are East-West oriented everywhere except near the pole.¹ The orientation

¹ In almost all cases, there is a 180° degeneracy in inferred impact direction. In rare cases (e.g. Schultz & Wrobel 2012), this degeneracy can be broken; we do *not* propose to study these rare cases.

distribution of the impact flux shows 200% deviations from isotropy (Fig. 2). If any of {obliquity, spin-axis location relative to the lithosphere, or the impactor inclination/eccentricity distribution} change, then the angles between impactors and the spin axis also change, causing a change in predicted orientation of elliptic craters. These 3 effects can be straightforwardly distinguished using a forward model (Fig. 1). Specifically:-

- (1) obliquity changes shift the proportion of N-S vs. E-W orientations at all latitudes (Fig. 1a), with longitudinal symmetry;
- (2) TPW unavoidably introduces a signature longitudinal ‘twist’ in the latitude-dependent preferred orientation of elliptical craters (Fig. 1b); the amplitude of the longitudinal twist is independent of obliquity (Schultz & Lutz-Garihan 1982), and has a diagnostic degree-2 order-2 symmetry (Matsuyama 2014);
- (3) Shifts in the distributions of bombarder orbits cause pinching and swelling of the amplitude of deviations from isotropy. To see this, consider an isotropic distribution of impactor relative-velocity vectors (as might occur if the bombarding population is the detritus from terrestrial-planet formation; Bottke & Norman 2017). In this limit (orange in Fig. 1c), the crater orientations are isotropic. Alternatively, consider impactors scattered from distant orbits (dark blue in Fig. 1c). The subset of the scattered population that impacts Mars will be drawn disproportionately from objects with high eccentricities and relatively modest inclinations. Relative-velocity vectors at the time of impact will be concentrated toward the ecliptic plane. Therefore, the the amplitude of the anisotropy of crater ellipticities will be large.

The bombarder-orbit uncertainty is not important for the last 3.0 Ga of Mars history, for which we expect that small bodies sourced from the asteroid belt are the main bombarders of Mars (Nesvorný et al. 2017). The Hungarias, which have high albedo, are only a minor contributor (~1%) to the impact flux at the present day (as for the past 3.0 Ga; note that the conclusions of Bottke et al. 2012 and Čuk 2012 have been significantly modified by the findings of Čuk & Nesvorný 2017).

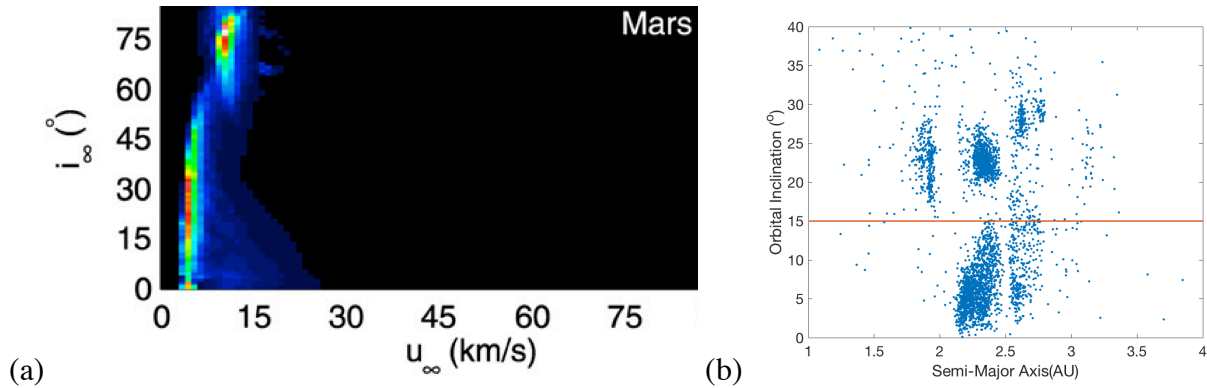
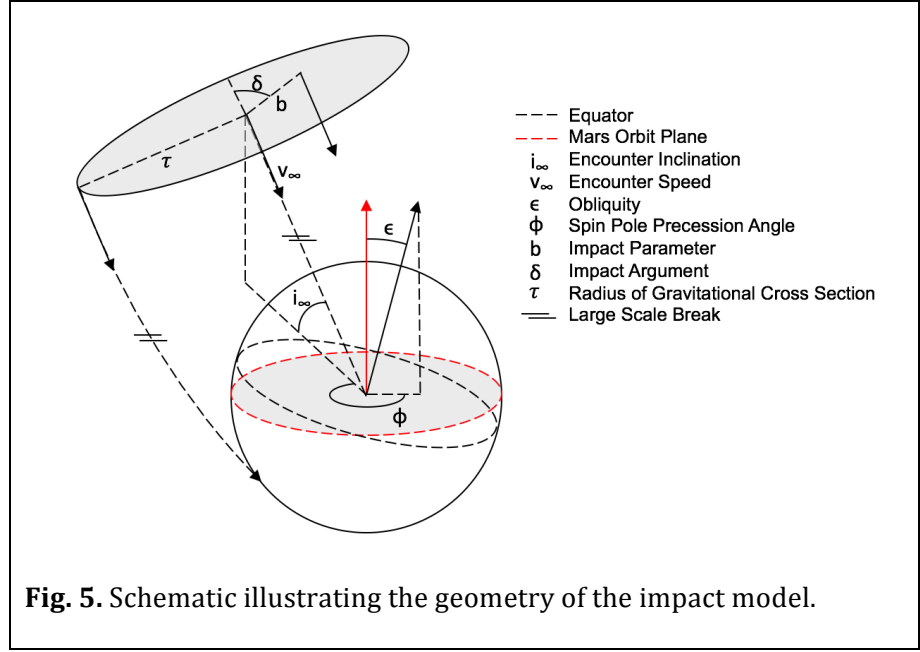


Fig. 4. (a) (From Le Feuvre & Weiczorek, 2008). Collision-probability heat map as a function of inclination (i_∞) and speed (u_∞) relative to the orbital plane of Mars (neither corrected for gravity focusing). High-energy impactors approach Mars from high ecliptic latitudes, lower-energy impactors approach Mars at moderate inclinations. As Mars’ obliquity is currently low, most craters above a given size on Mars today are formed by bolides approaching from high geographic latitudes. **(b)** (From Holo et al., in review). Orbital inclination vs. semi-major axis for Mars-crossing objects (from <https://www.minorplanetcenter.net/iau/MPCORB/MPCORB.DAT>).

For absolute magnitude $H < 16$, $n = 3282$.

None of this works unless the orientations of present-day craters faithfully preserve impact conditions. Remarkably, Noachian-terrain Mars craters (>80% of which formed in the Noachian) show the same ellipticity histogram as fresh Mars craters (Fig. 6). This strongly suggests that post-impact modification has not affected the orientations, because anisotropic post-impact



modification could only increase the fraction of craters at a given ellipticity (Fig. 6). Although glacial *deposits* within craters at high latitude are asymmetric, this has little effect on rim asymmetry (Conway & Mangold 2013). Indeed, the ellipticity histograms are very similar as a function of latitude (in contrast to the orientation histograms, which vary systematically with latitude). Therefore, present-day crater orientations are a good proxy for impact conditions.

Some early studies proposed that some elliptical craters on Mars resulted from inspiralling Mars-orbiting satellites and rings (Schultz & Lutz-Garihan 1982, Arkani-Hamed 2005). These early hypotheses, which predate the availability of large crater databases (Robbins & Hynek 2012), all predict one or more bands of elliptical craters that are tightly-collimated in (i) space, (ii) orientation, and (iii) ellipticity. These should be (respectively) (i) a great circle, (ii) E-W after TPW correction, and (iii) high and distinct from the background flux of circumsolar impactors. These predicted collimations have not been observed by us in the database of Robbins & Hynek (2012). Moreover, there is no trend to a greater frequency of higher ellipticity craters at lower latitudes (as might be expected for areocentric impactors with modest TPW). Moreover, theory predicts that inspiralling moons are tidally shredded and yield a ridge, not craters (Dombard et al. 2012, Black & Mittal 2015, Hesselbrock & Minton 2017, Fan & Kite 2018). For these three reasons, we do not think that inspiralling moons, if any existed, were a major contributor to the elliptical-crater orientation anisotropies on Mars. However, if we are wrong and moon-inspiral did in fact form a large fraction of the elliptical craters on Mars, then this would show up as an easy-to-diagnose residual in our analysis.

2.3.3. Preliminary work: We have validated the data, built a flexible code base, and already retrieved a key geologic parameter using the method.

We have mitigated the risk that might be associated with an unfamiliar method by (1) establishing the validity of the data, (2) establishing the usefulness of the approach through retrieving a key geologic parameter using the method, and (3) by building a code base that we can modify to invert for different geometric parameters.

Specifically, we developed a numerical forward model of the effect of obliquity on the orientations of elliptic craters using realistic ensembles of simulated Martian impactor orbits, and ~ 3.5 Gyr-long Martian obliquity simulations (from previous work) (Kite et al. 2015). We then used a validated version of a global database of Martian crater ellipticities and orientations (Robbins and Hynek 2012) and the ages of underlying geologic units (Tanaka et al. 2014) to invert for the true Martian obliquity history over the Late Hesperian and Amazonian.

(1) The dataset is complete, publicly available, and independently validated: The Robbins global Mars crater database ($>6 \times 10^5$ craters; Robbins and Hynek, 2012) contains measurements of crater ellipticities (ratio of major to minor axes lengths) and major axis orientations (absolute azimuth from due North) obtained from fitting ellipses to points traced around crater rims on a THEMIS base. For ellipticities >1.1 , long-axis orientation can be measured reliably for diameters $D > 3$ km ($>95\%$ per-crater confidence; Robbins & Hynek 2012). We have thoroughly checked the dataset for systematic errors. For example, we looked for latitude-bin-dependent lighting-angle effects and projection-related error, and did not find any. We also searched for systematic inter-analyst error. To do so, we divided the Robbins database into ellipticity-diameter bins, where ellipticity bins had a minimum value of 1.1 and width 0.1, and diameter bins had a minimum value of 5 km and $\sqrt{2}$ scaled widths. We randomly sampled up to 10 craters from each 2-D ellipticity-diameter bin in the database. We independently retraced these craters (which spanned a wide range of ellipticities, diameters, degradation states, and latitudes), removed projection effects, and fit ellipses to them using a direct non-linear least squares procedure (Fitzgibbon et al., 1999). We compared our measured ellipticities and orientations to those in the Robbins & Hynek (2012) database. The inter-analyst residuals (defined as the difference between the values measured by Robbins and Hynek (2012) and our re-measured values for each crater) had both a non-zero mean and a non-zero skewness. To assess whether these residuals can be attributed to random error, we resampled the residuals with replacement 10,000 times to produce a bootstrapped ensemble of equally likely residual distributions. Histograms of the bootstrapped means show that the inter-analyst residuals for both ellipticity and orientation have means (and skewnesses) that are not significantly different than zero (Fig. 7). We conclude that measurements of ellipticity and major-axis orientation show no systematic inter-analyst error. Restricting this analysis to craters with ($1.1 < \text{ellipticity} < 1.3$), as this is the region in which most of our final data lies, we found that orientation residual means and skewnesses are still not significantly different than 0. For craters with modest ellipticities, we found that the orientation residuals are roughly normally distributed ($\sigma = 5^\circ$). Thus, we conclude that the Robbins and Hynek (2012)

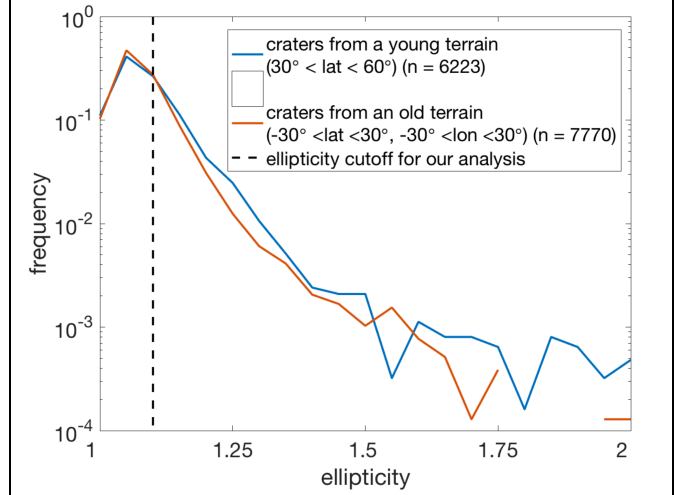


Fig. 6. The ellipticity histograms of fresh craters and ancient-terrain craters are the same within error, which demonstrates that anisotropic post-impact modification is minor (even for ancient craters). This excludes e.g. snowmelt-driven anisotropic erosion as a major contributor to N-S crater elongation.

database provides a suitable constraint on our modeling, with no systematic inter-analyst error and well-constrained random inter-analyst error.

(2) Establishing the usefulness of the approach:

We have demonstrated that this method can retrieve key geologic parameters for Mars in an analysis of relatively recent (<3.2 Gya) elliptical craters on Mars. These craters have long axes that are preferentially oriented N-S (Fig. 2). For the Amazonian and latest Hesperian, the orbital elements of the $\sim 10^3$ present-day Mars-Crossing Objects (MCOs) (Fig. 4) are statistically representative of the last-3.0 Gyr bombarding population. Therefore, the velocity vectors of the past impacting bodies can be approximated by sampling collisions from `mercury6` forward models sampling the present (MPCORB.dat, absolute magnitude $H \leq 14$) Mars-crossing objects. This forward-modeling procedure is described in detail in §2.4.1. We also found no evidence for large-amplitude net true polar wander (Kite et al. 2009). The only remaining variable is obliquity history. Because the Solar System is chaotic, planet obliquity cannot be deterministically reverse-

integrated beyond ~ 100 Mya. **Many geologic methods have been proposed to vault the fundamental barrier of the chaotic diffusion of the Solar System (e.g. Olson 1986, Martinez & Dera 2015, Ma et al. 2017), but all are indirect. Now we have a direct method.** In our preliminary study (Holo, Kite, and Robbins, in review) we found that the mean obliquity was lower than the central expectation from a $\sim 10^3$ -solar-system probabilistic ensemble (Kite et al. Icarus 2015), and ruled out higher mean obliquities (Fig. 8). Similarly, the percentage of time that Mars' obliquity was $>40^\circ$ was less than 50%.

(3) Risk of model development has been mitigated: We developed a forward model for the PDF of elliptic crater orientations on Mars that contains three major components: 1. An ensemble of possible Mars obliquity histories (described in Kite et al. 2015), 2. a long-term cratering model that, using a forward N-body simulation, estimates the locations, sizes and orientations of elliptic impact craters as a function of obliquity and 3. a resampling scheme that corrects the impact model for the effects of resurfacing by geologic processes (by forcing the predicted latitude-diameter distribution to the observed one) and maximum crater ages as constrained by ages of underlying geologic units (Fig. 3). Fitting this prediction to data in the now-vetted Robbins database allows us to constrain properties of the true Late Hesperian and Amazonian Mars obliquity history.

In summary, the preliminary shows (1) the validity of the data, (2) the reasonableness of the approach, and (3) a code base that we can modify to invert for different geometric parameters, as described below.

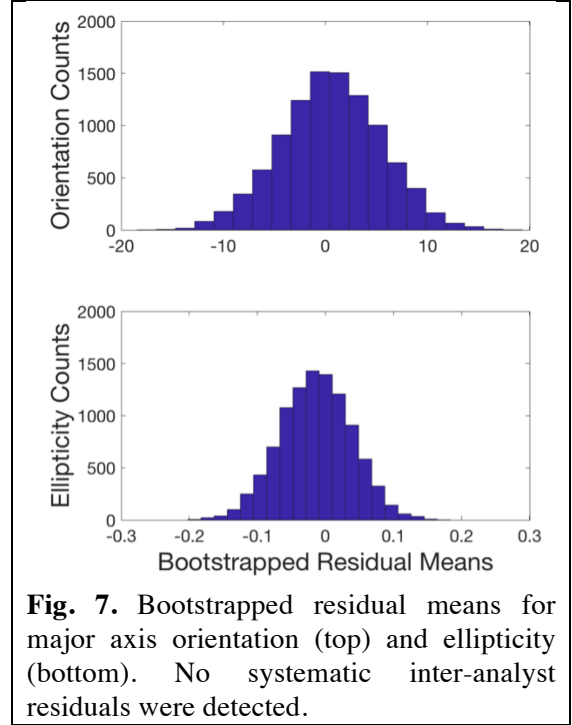


Fig. 7. Bootstrapped residual means for major axis orientation (top) and ellipticity (bottom). No systematic inter-analyst residuals were detected.

2.4 Technical Approach and Methodology.

2.4.1. Description of core model.

We propose to extend our analysis to more ancient (Noachian and Early Hesperian) craters on Mars. By comparison of the ancient craters to the young craters, we have already found that erosional modification of ancient craters (Howard 2007) has not significantly altered their ellipticities or orientations (Fig. 6). In the first part of the proposed work, we will quantify the paleopole for both the Late Hesperian - Amazonian time period and the Noachian - Early Hesperian time period. The results may or may not be consistent with the present pole. This will directly test claims of large-amplitude True Polar Wander on Mars. In the second part of the proposed work, we will marginalize over the unknown past obliquity to constrain the ancient impacting populations. Specifically, we will test (a) the "dregs of accretion" hypothesis, in which the ancient impacting population derives from the orbital annulus of the terrestrial planets; (b) the asteroid-belt source hypothesis; (c) the distant-source hypothesis (Table 1; Bottke & Norman 2017, and references therein). These 3 hypotheses make distinct predictions for the relative-velocity vectors of the objects striking Mars and thus for the orientations of the ancient elliptical impact craters.

The existing code for forward modeling of Late Hesperian and Amazonian elliptic crater orientations works as follows. First, the open-source N-body code `mercury6` (Chambers 1999) is used to generate collisions between Mars, and Mars-crossing objects drawn from the publicly-available MPCORB.dat file (<https://www.minorplanetcenter.net/iau/MPCORB.html>). We use $H \leq 14$ objects for which MPCORB.dat is likely close to complete (JeongAhn & Malhotra 2015). Orbits are integrated for ~ 10 Myr, and close encounters are considered to be collisions for the purposes of building up collision statistics. The run length is sufficient to average over the Mars eccentricity and nodal cycles (Jeong-Ahn & Malhotra 2015). No Mars-crosser is allowed to collide twice, and neither the high-inclination Mars-crossing population nor the low-inclination Mars-crossing population is significantly depleted during the course of the N-body run. The N-body runs are computationally inexpensive. The result from the N-body runs is a representative ensemble of encounter inclinations (relative to a Solar System reference plane) and speeds.

This output is ingested by a geometry script (Fig. 5). The output of this script is an ensemble of elliptic crater locations and diameters, as well as impactor velocity vectors at the time of impact, and the impact angle. To do this, the precise location of the impactor relative to Mars is randomized, and gravity focusing is included. Mars' rotation velocity (at the equator, 0.25 km/s) is neglected, because Mars' rotation speed is much smaller than the impactor velocities (>10 km/s including Mars escape velocity; Fig. 4a). The geometry script imposes a size-frequency distribution on the impactors; the size-frequency distribution is tuned to match the observed crater size-frequency distribution. In practice, almost no tuning is required. This is unsurprising, because published scalings relating crater size to impactor size and velocity incorporate information about crater size-frequency distributions. Crater diameter is computed as a function of impactor mass (using a mean-albedo assumption), impact velocity, and impact angle (Collins et al. 2011, Melosh 1989, Pierazzo & Melosh 2000). For modern Mars-crossers, inclination is positively correlated with speed (Fig. 4a), and so high-inclination objects make larger craters. 5×10^6 impactors are generated, and only impactors striking at the most shallow angles are retained (we use the shallowest 5%; the exact percentage is arbitrary, and does not affect the results).

Research is actively ongoing into the detailed physics of oblique impacts (e.g. Davison et al. 2011). Fortunately, the only piece of impact physics that is necessary to our method is that the long axes of elliptic craters are, on average, aligned with the impact relative-velocity vector. For example, at no point do we attempt to match the ellipticity histogram. This is not an impact-physics proposal.

A second geometry script takes the output ensemble (“pre-obliquity-impacts”), and, for each elliptic-crater-forming impact impact, considers obliquities ranging from 0° to 90° , in 1° intervals. For each combination, the velocity vectors are projected onto the planet's tangent plane, and the following key parameters are saved: latitude, diameter, and orientation of the resulting elliptic craters.

The forward model is next compared to the data. This is an “embarrassingly parallel” step, and is in fact parallelized (for convenience, not because of computational necessity) on the University of Chicago “Midway” cluster. To relate the geologic terrain ages to the absolute ages from the obliquity-integration ensemble, we bracket chronology uncertainty by applying the chronologies of both Neukum et al. (2001) and Hartmann (2005) (as tabulated by Michael 2013) (Fig. 8b). We load (1) the predicted/synthetic (forward-modeled) craters, as well as (2) a database of actual craters (the craters on Mars whose latitude-diameter distribution we want to match in our predictions), and also (3) candidate obliquity histories obtained from a previously-published, stochastic model of long-term obliquity evolution on Mars (Armstrong et al. 2004, Kite et al. 2015). Any realistic Mars obliquity history samples many obliquities (Touma & Wisdom 1993, Laskar et al. 2004). Different obliquities cause different crater orientations (Fig. 8a), and so the predicted crater-obliquity histogram for any candidate obliquity history is a (chronology-function-weighted) sum over history (Fig. 8b, dashed lines). There are >300 candidate obliquity histories in the ensemble, with a large variance in mean obliquity. Only Late Hesperian and Amazonian terrains are included. The data are then bootstrap-resampled and the frequency with which the bootstrapped data agree with each candidate obliquity history is recorded.

The computer requirements are well within the capabilities of resources controlled by the PI as documented in §8.2, Facilities and Equipment.

In §2.4.4, the basic workflow above is the same, but the forward models change in order to “float” the bombardier orbits.

2.4.2. Task 1: Determine TPW for the Amazonian and late Hesperian.

The hypotheses to be tested in this Task include the following. For the Amazonian and Late Hesperian, Perron et al. (2007) propose 30° - 60° polar wander based on Mars shorelines. Zuber (2007) proposes the emplacement of the Elysium volcanic province drove this TPW. Alternatively, Matsuyama and Manga (2010) infer a $<25^\circ$ upper limit on rotation, and Kite et al. (2009) and Scanlon et al. (2018) propose an even smaller ($<10^\circ$) twist.

The input crater dataset will be from Robbins and Hynek (2012). We exclude the largest basins, for which planetary curvature effects become important. After restricting for $D > 4$ km and ellipticity > 1.1 , we obtain 16575 craters. $D > 4$ km and ellipticity > 1.1 are chosen to be well above the sizes and ellipticities for which random tracing errors can corrupt the signal (Robbins & Hynek 2012). For the Late Hesperian and Amazonian we already know there is a N-S preference in crater orientations, corresponding to a low mean obliquity (Fig. 2).

The key to determining TPW is that craters can be preferentially oriented either E-W or N-S as a function of latitude (depending on obliquity; Fig. 8a), but this preferred orientation is longitudinally invariant in the absence of TPW. TPW introduces a longitudinal twist into the distribution (degree 2, order 2; Matsuyama 2014). Note that even for the obliquity = 45° case in Fig. 8a, there is still a strong grain due to differences (not shown) between high-latitude versus low-latitude mean orientations.

To test the TPW hypothesis, we will use elliptical crater orientations. The main practical difficulty is that a simple bootstrap cannot be used to obtain the paleopole, because Late Hesperian and Amazonian terrains are unevenly distributed across Mars. To mitigate this, for each of $360 \times 180 = 64800$ trial paleopoles, we will calculate what the preferred orientation should be in each $5^\circ \times 10^\circ$ tile containing at least one LH/A elliptic crater; the log-likelihoods of the data given the model will be combined to calculate the best-fitting pole and its error envelope (Mardia & Jupp 2000). If the error envelope does not overlap today's spin pole, then TPW is detected.

We will examine the sensitivity of our results to varying the D cutoff over the range 4-10 km, and the threshold ellipticity over the range 1.1-1.2. These ranges of threshold D and threshold ellipticity are justified by preliminary work (Fig. 2; Robbins & Hynek 2012).

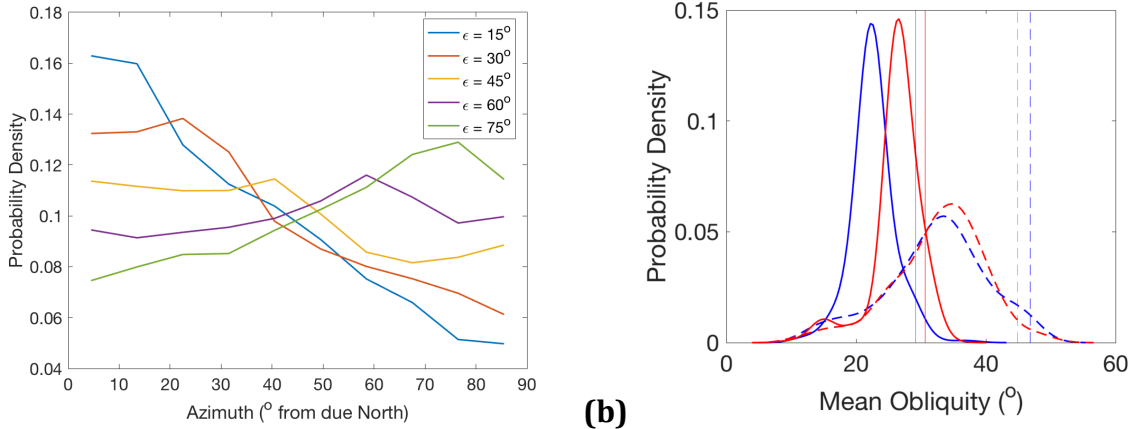


Fig. 8. (From Holo et al., in review) **(a)** Global elliptic crater azimuth PDF (9° bins) as a function of a single fixed obliquity prior to geologic correction. At low obliquities, there is a preference for North-South oriented elliptic craters. This trend is reversed at high obliquities (Fig. 1a). **(b)** Smoothed PDFs (Gaussian kernel, 2° bandwidth) of estimates of the mean obliquity. Results using Hartmann (2005) chronology are shown in blue, while results using the Neukum et al. (2001) chronology are shown in red. The dashed lines are the histogram of the 3.3-Gyr time-averaged obliquities from the individual runs in the obliquity-history ensemble (prior to model application), and the solid lines represent the bootstrapped retrieved value (posterior). Vertical lines show 97.5th percentile locations.

In the event that we find TPW inconsistent with zero for the Late Hesperian and Amazonian, then we will re-solve for Late Hesperian and Amazonian obliquity history, using the procedure in §2.4.1, after rotating coordinates to the retrieved paleopole.

2.4.3. Task 2. Constrain Mars TPW for the Noachian to Early Hesperian.

Building on Task 1, we will extend our analysis to Noachian terrains, which host craters that (on average) have more degraded topography. First, we will repeat the blind inter-analyst validation procedure described in §2.3.3 for 500 more-degraded craters, selected at random. For the validation step, crater degradation state will be identified using the depth/diameter ratio, following Forsberg-Taylor et al. (2004). This procedure will quantify inter-analyst scatter for Noachian craters. As part of this check, we will test for mirror symmetry about the N-S line of the picked orientations in 20° latitude bins for latitudes poleward of 20°N and S. This is a test for lighting-angle effects, which our preliminary work indicates will be small.

Only Noachian and Early Hesperian terrains will be used (using the GIS shapefiles of Tanaka et al. 2014 to exclude younger terrain). Although post-depositional modification of crater orientations is small overall (Fig. 6), a particular concern for Noachian terrains is tectonic distortion. Specifically, craters on Claritas Fossae are notably tectonically distorted. Therefore, we will exclude Claritas Fossae from our analysis. Away from the Tharsis-radial rifts, crater distortion is uncommon. This is because Mars tectonic strain is small, with rare exceptions (Andrews-Hanna et al. 2008).

The error analysis in the obliquity work (§2.3) was sufficient for that task, but a more precise analysis is rewarding for TPW. Specifically, we will check that the latitudinal trends in the data (N-S orientation strongest at higher latitude) are reproduced by the model. This is a strong test of the model, because the latitudinal trends are highly statistically significant. Next, we will double-check the crater validation using CTX imagery, to verify that crater ellipticities are not biased by the use of THEMIS imagery in our dataset. We will also (for Noachian craters) use spatial clustering analysis (Michael et al. 2012) to check for doublet/multiple fragment craters (e.g. Melosh & Schenk 1993), and combine any doublets/multiplerts for the purposes of assessing statistical significance.

2.4.4. Task 3. Constrain bombardier orbits for the Noachian to Early Hesperian.

Claims about early Mars bombardier source orbits, to be tested by the proposed investigation:

Hypothesis A. Planetesimal leftovers from Mars accretion (Morbidelli et al. 2001, Bottke et al. 2007). For the purposes of this proposal, re-accreting ejecta from a giant impact on Mars (Minton et al. 2015) is a special case of Hypothesis A.

Hypothesis B. Escapees from the young asteroid belt (Walsh et al. 2011, Morbidelli et al. 2015, Nesvorný et al. 2017). For the purposes of this proposal, destruction of a large asteroid (or destruction/destabilization of a fifth terrestrial planet) at or near the current location of the asteroid belt is a special case of hypothesis B.

Hypothesis C. Ancestral Kuiper belt. Modern variations (e.g. Morbidelli et al. 2015) on the Nice model (Gomes et al. 2005, Walsh et al. 2011).

Other ideas, such as destabilization of objects in the vicinity of Jupiter's orbit or between Jupiter and Saturn, are intermediate between Hypotheses B and C.

Table 1. Selected subset of claims about early Mars bombardier source orbits, to be tested by the proposed investigation (Bottke & Norman 2017). See Fig. 1 for principle of test.

For the Noachian to Early Hesperian time window (which is dominated by Noachian-aged craters; Irwin et al. 2013), we will test the hypotheses listed in Table 1 by (a) running `mercury6` forward models with 5,000 test-particle bombarders in order to generate a set of impactor relative-velocity vectors, (b) passing the impactor relative-velocity vectors through our pipeline (§2.4.1) to generate obliquity-and-latitude dependent predictions for Noachian elliptical-crater orientations, (c) marginalizing over obliquity and comparing to data.

The initial conditions for our 10-Myr-long `mercury6` forward models will vary the following three key parameters, for a total of $4 \times 2 \times 2 = 16$ forward models.

- **Bombarder orbits:** The semimajor axes for bombarders will be varied between the forward models. Semimajor-axis ranges of 1.52 ± 0.23 AU, 2.3 ± 0.35 AU, 5 ± 2 AU, and 20 ± 5 AU will be (separately) considered, corresponding (respectively) to hypotheses A, B, and two variations on hypothesis C, from Table 1. Following Kite & Ford (2018), the initial orbital eccentricities and inclinations will be drawn from Rayleigh distributions, with Rayleigh parameters set to ensure that (a) eccentricity and inclination are equally excited (this is conservative for the purposes of ruling out hypotheses about bombarder origin), and (b) a large fraction of the bombarders cross Mars. The three remaining angles, argument of pericenter, longitude of ascending node, and mean anomaly, will each be drawn from uniform distributions ($0 \leftrightarrow 2\pi$).
- **Mars eccentricity:** Mars eccentricity is poorly constrained for the Noachian (e.g. Agnor & Lin 2012); to bracket this uncertainty, we will consider an initial Mars eccentricity of zero, and also an initial Mars eccentricity equal to that of today’s Mars.
- **Circular Jupiter+Saturn versus Eccentric Jupiter+Saturn:** We will consider a Jupiter and Saturn with eccentricity equal to today’s Jupiter+Saturn, and also an initial Jupiter+Saturn eccentricity of zero. For the second case, Jupiter+Saturn will be moved to semimajor axes appropriate for Nice-model-like initial conditions (Morbidelli et al. 2015).

The initial orbital parameters for the other planets will be the same as today. There will be no migration in the model runs. We will consider two obliquity options for marginalization: (i) an obliquity pdf that is structured by the current architecture of the Solar System (Laskar et al. 2004, Kite et al. 2015); (ii) a lower-obliquity pdf (Brasser & Walsh 2011) corresponding to one hypothetical pre-LHB Solar System architecture. (It is also possible that our analysis will be able to constrain Noachian obliquity directly, although we cannot guarantee this).

These straightforward and relatively brief N-body simulations cannot provide, and are not intended to provide, complete candidate Solar System histories. Rather, they will provide reasonable internally-consistent sets of candidate Noachian-impactor relative-velocity vectors.

For comparison of the model to data, we will use two approaches to get Noachian and Early Hesperian craters. The simplest is to consider only craters on Noachian and Early Hesperian terrains. This will include a small fraction of Late Hesperian and Amazonian craters. To get the best possible constraint on bombarder source, we will use a refined method to remove this small fraction of contaminants. Specifically, we will use crater depth/diameter ratio, normalized for diameter, as a proxy for age. This is a widely used procedure (Mangold et al 2012, Craddock & Howard 2002, Forsberg-Taylor et al. 2004, Irwin et al. 2013). Out of an abundance of caution, to test this assumption, we will compare a fit using only craters on young terrains (which are certain to be young) to a fit using only fresh-appearing craters on old terrains. If the fits disagree beyond

statistical error, then the assumption of crater degradation state as a proxy for age is questionable, and we would then revert to the simplest approach of considering all craters on Noachian and Early Hesperian terrains.

For each of the 16 forward models, we will report data-model mismatch (χ^2 in orientation), and qualitative fit or misfit relative to latitude trends in preferred orientation. We plan to advance on Task 3 in parallel with Task 2. However, if Task 2 finds a paleopole different from today's pole, then it is easy to propagate this paleopole through the data-model mismatch calculation.

2.4.5. Assumptions and limitations.

It is worth emphasizing the assumptions driving the design of our modeling approach. (1) Although most published bombarder-source hypotheses predict distinct elliptical-crater orientations, we cannot exclude a high- e bombarder-population from the innermost solar system. This is acceptable, because no published model predicts that the bombarder source was the innermost solar system. (2) Our method constrains long-term average True Polar Wander and is insensitive to excursions of Mars' spin pole that are *rapid, rapidly reversed, and have cumulatively short duration* (an unlikely combination for Mars-like planets; Tsai & Stevenson 2007, Creveling et al. 2012, Rose & Buffett 2017). In this respect, our data-driven constraint on slow net true polar wander will be complementary to theoretical “speed limits” on polar wander that argue against rapid polar wander. Given a long and complicated random-walk loading history, it is implausible that large gross TPW would give small net TPW. (3) Neither our technique, nor most of the methods shown in Fig. 3, can discriminate TPW from net lithospheric rotation (NLR). This is an unavoidable limitation for any method that uses surface markers to track TPW – for example it also applies to Earth paleomagnetic methods, the “gold standard” for retrieving TPW. The effects of TPW and NLR for most purposes are the same. (4) Our data consist of impact craters recognizable on today's surface (Robbins & Hynes 2012). This crater population would be reset by the Borealis impact. Therefore, processes predating the age of the Borealis impact (estimated at 4.3 Ga by Andrews-Hanna & Bottke 2017, but with large uncertainty) cannot be probed by our method. Note that the dynamo remained active after Borealis (e.g. Stanley et al. 2008). It is possible that (for example) the delivery of highly-siderophile elements to Earth's mantle predates Borealis. Therefore, our method is not a panacea for inner-solar-system volatile delivery problems, but remains complementary to existing methods, such as geochemistry and N-body simulations. (5) Our analysis averages over the Noachian and Early Hesperian; this is a simplification, because both the spin-pole and the bombarder source likely changed over time. Both TPW and bombarder populations on Mars had a long and presumably complex history; we propose to test simple hypotheses about that history, with an eye to enabling richer hypotheses and tests in future.

2.5. Perceived Impact of the Proposed Work.

The proposed modeling will advance the state-of-the-art by applying a basic geometric method (the elliptical-crater orientation proxy) that has not previously been applied to heliocentric impactors. The proposed work will directly test claims (Fig. 3) of large-amplitude true polar wander on Mars. If the TPW hypothesis fails the test at Mars, this will have an impact on paleoclimate reconstruction, Mars geodynamics/geophysics research, and indirectly call into question the subset of claims for large-amplitude true polar wander elsewhere in the Solar System that are based on the methods in Fig. 3. The question of the source of the “Late Heavy Bombardment” impactors has excited planetary scientists for over 40 years; in the most recent

review of of the LHB, Bottke & Norman (2017) write “The LHB literature is so vast that no single article can comprehensively summarize it all.” The source region of the LHB is important in part because it may overlap with the source region for late-arriving terrestrial-planet volatiles (e.g. Morbidelli et al. 2000, Dauphas & Morbidelli 2014, and references therein). Indeed, the failure to converge on a consensus interpretation of the LHB is part of the motivation for the (New Frontiers Program) South Pole Aitken Sample Return and the (Discovery Program) *Lucy* mission; the latter has been selected for flight. Therefore, existing methods might benefit from an independent constraint, such as the one proposed here. The proposed work opens up a new and independent approach to the problem of the source of the ancient impactors, a problem that so far has been tackled largely using geochemical methods. Mars is a test-bed for developing the elliptical-crater anisotropy proxy, and this proxy can also be applied to other worlds. Examples include (most immediately) the Moon, for which a large database of craters is nearing completion (Robbins 2017), and also Mercury, Ceres, and Vesta.

The Relevance Statement for this proposal is included on the cover page as requested in Appendix C.3 of the NRA.

2.6. Work Plan.

	Activities/milestones.	Products.
Year 1.	<ul style="list-style-type: none">• Complete error-quantification for post-3.3 Ga craters.• Validate pre-3.3 Ga crater orientations.• Build TPW-code.• Apply TPW-code to post-3.3 Ga TPW.	<ul style="list-style-type: none">✓ LPSC presentation on: Elliptical-crater orientations data description.✓ JGR-length paper on data description and post-3.3 Ga TPW.
Year 2.	<ul style="list-style-type: none">• Apply TPW-code to pre-3.3 Ga TPW.• Start writing bombarder-orbit quantification code.• Check for obliquity-TPW tradeoffs; error analysis.• Begin to upload data to repositories as specified in DMP.	<ul style="list-style-type: none">✓ LPSC presentation on: Model description, emphasizing TPW retrieval.✓ GRL-length paper on TPW through the ages on Mars and implications for geophysics and climate.
Year 3.	<ul style="list-style-type: none">• Complete bombarder-orbit quantification code.• Apply bombarder-orbit quantification code.• Continue to upload data to repositories as specified in DMP.	<ul style="list-style-type: none">✓ LPSC presentation on: Bombarder-orbit constraints.✓ JGR-length paper on bombarder orbit constraints, implications for the early history of the Solar System.

Productivity on past SSW grants with Kite as PI is as follows: NNX15AH98G, 3 papers submitted in 3 years; NNX16AG55G, 5 papers submitted in 2 years.

2.7. Personnel and Qualifications. (For FTE information, see §6, Budget Justification).

PI **Edwin Kite** is an assistant professor at the University of Chicago (UChicago). As PI, he will participate in all aspects of the proposed work and oversee its implementation. Collaborator **Stuart Robbins** is a research scientist at SwRI Boulder. He will advise and consult on the use of his database of elliptical crater orientations, and will contribute his expertise to the interpretation of the results. Collaborator **David Minton** is an assistant professor at Purdue University and expert in N-body modeling and the “Late Heavy Bombardment.” He will consult with the PI on the selection of input parameters for N-body modeling, and the interpretation of the results. A **University of Chicago graduate student** (to be identified) will validate the crater database, extend the model to include TPW and bombarder-orbits, and carry out the retrievals, as part of their PhD research.

3. References.

- Agnor, Craig B.; Lin, D. N. C., 2012, On the Migration of Jupiter and Saturn: Constraints from Linear Models of Secular Resonant Coupling with the Terrestrial Planets, *The Astrophysical Journal*, Volume 745, Issue 2, article id. 143, 20 pp. (2012).
- Andrews-Hanna, Jeffrey C.; Zuber, Maria T.; Hauck, Steven A., 2008, Strike-slip faults on Mars: Observations and implications for global tectonics and geodynamics, *Journal of Geophysical Research*, Volume 113, Issue E8, CiteID E08002.
- Arkani-Hamed, Jafar, 2001, Paleomagnetic pole positions and pole reversals of Mars, *Geophysical Research Letters*, Volume 28, Issue 17, p. 3409-3412.
- Arkani-Hamed, Jafar, 2009, Polar wander of Mars: Evidence from giant impact basins, *Icarus*, Volume 204, Issue 2, p. 489-498.
- Armstrong, John C.; Leovy, Conway B.; Quinn, Thomas, 2004, A 1 Gyr climate model for Mars: new orbital statistics and the importance of seasonally resolved polar processes, *Icarus*, Volume 171, Issue 2, p. 255-271. (Describes obliquity model).
- Batygin, Konstantin; Laughlin, Greg, 2015, Jupiter's decisive role in the inner Solar System's early evolution, *Proceedings of the National Academy of Sciences*, vol. 112, issue 14, pp. 4214-4217.
- Bills, B.G., 2006, Non-Chaotic Obliquity Variations of Mars, *Lunar and Planetary Science Conference*, abstract #2093.
- Black, BA, and T Mittal, 2015, The demise of Phobos and development of a Martian ring system, *Nature Geoscience* 8 (12), 913-917
- Botke, William F.; Andrews-Hanna, Jeffrey C., 2017, A post-accretionary lull in large impacts on early Mars, *Nature Geoscience*, Volume 10, Issue 5, pp. 344-348.
- Botke, William F., Jr.; Rubincam, David P.; Burns, Joseph A., 2000a, Dynamical Evolution of Main Belt Meteoroids: Numerical Simulations Incorporating Planetary Perturbations and Yarkovsky Thermal Forces, *Icarus*, Volume 145, Issue 2, p. 301-331.
- Botke, W.F., Love, S.G., Tytell, D., and Glotch, T., 2000b, Interpreting the Elliptical Crater Populations on Mars, Venus, and the Moon, *Icarus*, 145-1, p. 108-121.
- Botke, W.F., Morbidelli, A., Jedicke, R., Petit, J-M, Levison, H.F., Michel, P., Metcalfe, T.S., 2002, Debiased Orbital and Absolute Magnitude Distribution of the Near-Earth Objects, *Icarus*, 156-2, p. 399-433.

- Bottke WF, Levison HF, Nesvorny D, Dones L. 2007. Can planetesimals left over from terrestrial planet formation produce the lunar Late Heavy Bombardment? *Icarus* 190(1):203–23.
- Bottke, W. F., Vokrouhlicky, D., Minton, D., Nesvorny, D., Morbidelli, A., Brasser, R., Simonson, B., Levison, H. F., 2012. An Archaean heavy bombardment from a destabilized extension of the asteroid belt. *Nature* 485, p. 78–81.
- Bouley, Sylvain; Baratoux, David; Matsuyama, Isamu; Forget, Francois; Séjourné, Antoine; Turbet, Martin; Costard, Francois, 2016, Late Tharsis formation and implications for early Mars, *Nature*, Volume 531, Issue 7594, pp. 344-347.
- Brasser, Ramon; Walsh, Kevin J., 2011, Stability analysis of the martian obliquity during the Noachian era, *Icarus*, Volume 213, Issue 1, p. 423-427.
- Brownlee, D., 2014, The Stardust Mission: Analyzing Samples from the Edge of the Solar System, *Annual Review of Earth and Planetary Sciences* 2014 42:1, 179-205.
- Ćuk, M., 2012, Chronology and Sources of Lunar Impact Bombardment, *Icarus*, 218, 69-79.
- Ćuk, M. and Nesvorny, D., 2017, Planetary Chaos and the (in)stability of Hungaria Asteroids, arXiv:1704.05552
- Chambers, J.E., 1999, A Hybrid Symplectic Integrator that Permits Close Encounters between Massive Bodies, *Monthly Notices of Royal Astron. Soc.*, 304, 793-799.
- Citron, Robert I., Michael Manga, and Douglas J. Hemingway, Timing of oceans on Mars from shoreline deformation, accepted.
- Collins, G.S., Elbeshausen, D., Davison, T.M., Robbins, S.J., Hynek, B.M., 2011, The size-frequency distribution of elliptical impact craters, *Earth and Planetary Science Letters*, 310-1, p. 1-8.
- Conway, Susan J.; Mangold, Nicolas, 2013, Evidence for Amazonian mid-latitude glaciation on Mars from impact crater asymmetry, *Icarus*, Volume 225, Issue 1, p. 413-423.
- Creveling, J. R.; Mitrovica, J. X.; Chan, N.-H.; Latychev, K.; Matsuyama, I., 2012, Mechanisms for oscillatory true polar wander, *Nature*, Volume 491, Issue 7423, pp. 244-248.
- Dauphas, Nicolas; Morbidelli, Alessandro, 2014, Geochemical and planetary dynamical views on the origin of Earth's atmosphere and oceans, in *Treatise on Geochemistry*, 2nd edition, arXiv:1312.1202
- Davison, Thomas M.; Collins, Gareth S.; Elbeshausen, Dirk; Wünnemann, Kai; Kearsley, Anton, 2011, Numerical modeling of oblique hypervelocity impacts on strong ductile targets, *Meteoritics & Planetary Science*, Volume 46, Issue 10, pp. 1510-1524.

- Fan, B., & Kite, E.S., “Upper limit on a paleo-equatorial ridge from a tidally-disrupted moon of Mars,” 49th Lunar and Planetary Science Conference, abstract #1054.
- Fassett CI, Minton DA. 2013. Impact bombardment of the terrestrial planets and the early history of the Solar System. *Nat. Geosci.* 6:520–24.
- Fassett, C.I., Levy, J.S., Dickson J.L., Head, J.W., 2014, An extended period of episodic northern mid-latitude glaciation on Mars during the middle to late Amazonian: Implications for long-term obliquity history, *Geology*, 42-9, p. 763-766.
- Fastook, J.L., Head, J.W., Marchant, D.R., Forget, F., Madeleine, J-B., 2012, Early Mars climate near the Noachian-Hesperian boundary: Independent evidence for cold conditions from basal melting of the south polar ice sheet (Dorsa Argentea Formation) and implications for valley network formation, *Icarus*, 219, p. 25-40.
- Fitzgibbon, A., M. Pilu, R. B. Fisher, 1999, Direct least square fitting of ellipses, *IEEE Trans. Pattern Anal. Mach. Intell.*, 21-5, p. 476–480.
- Forget, F.; Haberle, R. M.; Montmessin, F.; Levrard, B.; Head, J. W., 2006, Formation of Glaciers on Mars by Atmospheric Precipitation at High Obliquity, *Science*, Volume 311, Issue 5759, pp. 368-371.
- Forsberg-Taylor, Nancy K.; Howard, Alan D.; Craddock, Robert A., 2004, Crater degradation in the Martian highlands: Morphometric analysis of the Sinus Sabaeus region and simulation modeling suggest fluvial processes, *Journal of Geophysical Research*, Volume 109, Issue E5, CiteID E05002.
- Frawley, James J.; Taylor, Patrick T., 2004, Paleo-pole positions from martian magnetic anomaly data, *Icarus*, Volume 172, Issue 2, p. 316-327.
- Gomes, R.; Levison, H. F.; Tsiganis, K.; Morbidelli, A., 2005, Origin of the cataclysmic Late Heavy Bombardment period of the terrestrial planets, *Nature*, Volume 435, Issue 7041, pp. 466-469.
- Grimm, R. E.; Solomon, S. C., 1986, Tectonic tests of proposed polar wander paths for Mars and the moon, *Icarus* (ISSN 0019-1035), vol. 65, Jan. 1986, p. 110-121.
- Grimm, R. E., K. P. Harrison, D. E. Stillman, M. R. Kirchoff, 2017, On the secular retention of ground water and ice on Mars, *JGR Planets*, 122, p. 94–109.
- Harada, Y., 2012, Long-term polar motion on a quasi-fluid planetary body with an elastic lithosphere: Semi-analytic solutions of the time-dependent equation, *Icarus*, Volume 220, Issue 2, August 2012, Pages 449-465.

- Hartmann, William K., 2005, Martian cratering 8: Isochron refinement and the chronology of Mars, *Icarus*, Volume 174, Issue 2, p. 294-320.
- Holo, S., Kite, E.S., & Robbins, S.J., “Mars obliquity history constrained by elliptic crater orientations,” moderate revisions requested by Earth and Planetary Science Letters.
- Hood, Lon L.; Young, Corryn N.; Richmond, Nicola C.; Harrison, Keith P., 2005, Modeling of major martian magnetic anomalies: Further evidence for polar reorientations during the Noachian, *Icarus*, Volume 177, Issue 1, p. 144-173.
- Howard, Alan D., 2007, Simulating the development of Martian highland landscapes through the interaction of impact cratering, fluvial erosion, and variable hydrologic forcing, *Geomorphology*, Volume 91, Issue 3-4, p. 332-363.
- Hynek, Brian M.; Robbins, Stuart J.; Šrámek, Ondřej; Zhong, Shijie J., 2011, Geological evidence for a migrating Tharsis plume on early Mars, *Earth and Planetary Science Letters*, Volume 310, Issue 3, p. 327-333.
- Irwin, Rossman P.; Tanaka, Kenneth L.; Robbins, Stuart J., 2013, Distribution of Early, Middle, and Late Noachian cratered surfaces in the Martian highlands: Implications for resurfacing events and processes, *Journal of Geophysical Research: Planets*, Volume 118, Issue 2, pp. 278-291
- Jakosky, B.M., & Carr, M.H., 1985, Possible precipitation of ice at low latitudes of Mars during periods of high obliquity, *Nature*, 315, p. 559-561.
- Jakosky, Bruce M.; Henderson, Bradley G.; Mellon, Michael T., 1995, Chaotic obliquity and the nature of the Martian climate, *Journal of Geophysical Research (ISSN 0148-0227)*, vol. 100, no. E1, p. 1579-1584.
- JeongAhn, Y., Malhotra, R., 2015, The current impact flux on Mars and its seasonal variation, *Icarus*, 262, p. 140-153
- Keane, James T.; Matsuyama, Isamu; Kamata, Shunichi; Steckloff, Jordan K., 2016, Reorientation and faulting of Pluto due to volatile loading within Sputnik Planitia, *Nature*, Volume 540, Issue 7631, pp. 90-93 (2016).
- Kite, E.S., Matsuyama, I., Manga, M., Perron, J.T., and Mitrovica, J.X., 2009, True polar wander driven by late-stage volcanism and the distribution of paleopolar deposits on Mars, *Earth and Planetary Science Letters*, 280, 254-267.
- Kite, E.S., Halevy, I., Kahre, M.A., Wolff, M.J., Manga, M., 2013, Seasonal melting and the formation of sedimentary rocks on Mars, with predictions for the Gale Crater mound. *Icarus*, 223, p. 181-210.

- Kite, E.S., Howard, A.D., Lucas, A.S., Armstrong, Aharonson, O. and Lamb, M.P., 2015, Stratigraphy of Aeolis Dorsa, Mars: stratigraphic context of the great river deposits, *Icarus*, 253, p. 223-242. (Describes 3.5-Gyr-long N-body calculations).
- Kite, E.S., & Ford, E., Habitability of exoplanet waterworlds, arXiv:1801.00748.
- Kobayashi, Daisuke; Sprenke, Kenneth F., 2010, Lithospheric drift on early Mars: Evidence in the magnetic field, *Icarus*, Volume 210, Issue 1, p. 37-42.
- Kreslavsky, M.A., and Head, J.W., 2005, Mars at very low obliquity: Atmospheric collapse and the fate of volatiles, *Geophys. Res. Lett.*, 32.
- Langlais, Benoit; Purucker, Michael, 2007, A polar magnetic paleopole associated with Apollinaris Patera, Mars, *Planetary and Space Science*, Volume 55, Issue 3, p. 270-279.
- Langlais, Benoit; Quesnel, Yoann, 2008, New perspectives on Mars' crustal magnetic field, *Comptes Rendus Geoscience*, v. 340, iss. 12, p. 791-800.
- Laskar, J. and Robutel, P., 1993, The chaotic obliquity of the planets, *Nature*, 361, p. 608-612.
- Laskar, J., Correia, A.C.M, Gastineau, M., Joutel, F., Levrard, B., Robutel, P., 2004, Long term evolution and chaotic diffusion of the insolation quantities of Mars, *Icarus* 170, p. 343-364.
- Li, G., and Batygin, K., 2014, On the spin-axis dynamics of a moonless Earth, *Astrophys. J.*, 790-69.
- Lissauer, J.J., Barnes, J.W., and Chambers, J.E., 2012, Obliquity variations of a moonless Earth, *Icarus*, 217, p. 77-87.
- Le Feuvre, M., Wieczorek, M.A., Nonuniform cratering of the terrestrial planets, *Icarus*, 2008, 197-1, p. 291-306.
- Ma, Chao; Meyers, Stephen R.; Sageman, Bradley B., 2017, Theory of chaotic orbital variations confirmed by Cretaceous geological evidence, *Nature*, Volume 542, Issue 7642, pp. 468-470.
- Mardia, K.V., and P.E. Jupp, 2000, *Directional statistics*, Wiley.
- Martinez, Mathieu; Dera, Guillaume, 2015, Orbital pacing of carbon fluxes by a ~9-My eccentricity cycle during the Mesozoic, *Proceedings of the National Academy of Sciences*, Volume 112, Issue 41, 2015, pp.12604-12609
- Matsuyama, I., and M. Manga, 2010, Mars without the equilibrium rotational figure, Tharsis, and the remnant rotational figure, *JGR*, 115.

- Matsuyama, Isamu; Nimmo, Francis; Mitrovica, Jerry X., 2014, Planetary Reorientation, Annual Review of Earth and Planetary Sciences, vol. 42, p.605-634.
- Melosh H. J. 1980. Tectonic patterns on a reoriented planet: Mars. *Icarus* 44:745–51.
- Melosh, H. J., 1989, Impact cratering: A geologic process, New York, Oxford University Press (Oxford Monographs on Geology and Geophysics, No. 11), 253 p.
- Melosh, H. J.; Schenk, P., 1993, Split comets and the origin of crater chains on Ganymede and Callisto, *Nature*, Volume 365, Issue 6448, pp. 731-733.
- Michael, G. G.; Platz, T.; Kneissl, T.; Schmedemann, N., 2012, Planetary surface dating from crater size-frequency distribution measurements: Spatial randomness and clustering, *Icarus*, Volume 218, Issue 1, p. 169-177.
- Milbury, C.; Schubert, G., 2010, Search for the global signature of the Martian dynamo, *Journal of Geophysical Research*, Volume 115, Issue E10, CiteID E10010.
- Minton, D. A.; Jackson, A. P.; Asphaug, E.; Fassett, C. I.; Richardson, J. E., 2015, Debris from Borealis Basin Formation as the Primary Impactor Population of Late Heavy Bombardment, Workshop on Early Solar System Impact Bombardment III, held 4-5 February, 2015 in Houston, Texas. LPI Contribution No. 1826, p.3033.
- Morbidelli, A.; Chambers, J.; Lunine, J. I.; Petit, J. M.; Robert, F.; Valsecchi, G. B.; Cyr, K. E., 2000, Source regions and time scales for the delivery of water to Earth, *Meteoritics & Planetary Science*, vol. 35, no. 6, pp. 1309-1320.
- Morbidelli A, Petit J-M, Gladman B, Chambers J. 2001. A plausible cause of the late heavy bombardment. *Meteorit. Planet. Sci.* 36:371–80
- Morbidelli A, Walsh KJ, O'Brien DP, Minton DA, Bottke WF. 2015. The dynamical evolution of the asteroid belt. In *Asteroids IV*, ed. P Michel, F DeMeo, WF Bottke, pp. 493–508. Tucson: Univ. Ariz. Press
- Nesvorny, D., Roig, F., & Bottke, W. F. 2017, Modeling the historical flux of planetary impactors, *Astronomical Journal*, 153, 103.
- Neukum, G.; Ivanov, B. A.; Hartmann, W. K., 2001, Cratering Records in the Inner Solar System in Relation to the Lunar Reference System, *Space Science Reviews*, v. 96, Issue 1/4, p. 55-86.
- Niles, Paul B.; Michalski, Joseph, 2009, Meridiani Planum sediments on Mars formed through weathering in massive ice deposits, *Nature Geoscience*, Volume 2, Issue 3, pp. 215-220.
- Nimmo, Francis; Pappalardo, Robert T., 2006, Diapir-induced reorientation of Saturn's moon

Enceladus, *Nature*, Volume 441, Issue 7093, pp. 614-616.

Olsen, P.E., 1986, A 40-million-year lake record of early Mesozoic orbital climatic forcing, *Science* 234 (4778), 842-848.

Orgel, Csilla, Gregory Michael, Caleb I. Fassett, Carolyn H. van der Bogert, Christian Riedel, Thomas Kneissl, Harald Hiesinger, Ancient bombardment of the inner Solar System - Reinvestigation of the “fingerprints” of different impactor populations on the lunar surface, *JGR Planets*, Accepted manuscript online: 6 February 2018.

Palucis, M.C., Dietrich, W.E., Hayes, A.G., Williams, R.M.E., Gupta, S., Mangold, N., Newsom, H., Hardgrove, C., Calef III, F., Sumner, D.Y., 2014, The origin and evolution of the Peace Vallis fan system that drains to the Curiosity landing area, Gale Crater, Mars, *JGR*, 199, p. 705-728.

Perron, J. Taylor; Mitrovica, Jerry X.; Manga, Michael; Matsuyama, Isamu; Richards, Mark A., Evidence for an ancient martian ocean in the topography of deformed shorelines, *Nature*, Volume 447, Issue 7146, pp. 840-843.

Phillips, R.J., et al., 2011, Massive CO₂ ice deposits sequestered in the south polar layered deposits of Mars, *Science*, 332, p. 838-841.

Pierazzo, E.; Melosh, H. J., 2000, Understanding Oblique Impacts from Experiments, Observations, and Modeling, *Annual Review of Earth And Planetary Sciences*, Volume 28, pp. 141-167.

Robbins, S. J. 2014. New crater calibrations for the lunar crater-age chronology. *Earth and Planetary Science Letters*, 403, p. 188-198.

Robbins, S. J. and B. M. Hynek, 2012, A new global database of Mars impact craters > 1 km: 1. Database creation, properties, and parameters. *JGR (Planets)* 117.

Robbins, S. J., 2017, A Global Lunar Crater Database, Complete for Craters ≥ 1 km, II, 48th Lunar and Planetary Science Conference, held 20-24 March 2017, at The Woodlands, Texas. LPI Contribution No. 1964, id.1631.

Roberts, James H.; Zhong, Shijie, 2007, The cause for the north south orientation of the crustal dichotomy and the equatorial location of Tharsis on Mars, *Icarus*, Volume 190, Issue 1, p. 24-31.

Roig F, Nesvorny D, Desouza SR. 2016. Jumping Jupiter can explain Mercury’s orbit. *Astrophys. J. Lett.* 820(2):L30

Rose, Ian; Buffett, Bruce, 2017, Scaling rates of true polar wander in convecting planets and moons, *Physics of the Earth and Planetary Interiors*, Volume 273, p. 1-10.

- Rouby, Hélène; Greff-Lefftz, Marianne; Besse, Jean, 2008, Rotational bulge and one plume convection pattern: Influence on Martian true polar wander, *Earth and Planetary Science Letters*, Volume 272, Issue 1-2, p. 212-220.
- Scanlon, K. E.; Head, J. W.; Fastook, J. L.; Wordsworth, R. D., 2018, The Dorsa Argentea Formation and the Noachian-Hesperian climate transition, *Icarus*, Volume 299, p. 339-363.
- Schenk, Paul; Matsuyama, Isamu; Nimmo, Francis, 2008, True polar wander on Europa from global-scale small-circle depressions, *Nature*, Volume 453, Issue 7193, pp. 368-371.
- Schlichting, Hilke E.; Mukhopadhyay, Sujoy, 2018, Atmosphere Impact Losses, *Space Science Reviews*, Volume 214, Issue 1, article id. #34, 31 pp.
- Schultz, P. H.; Lutz-Garihan, A. B., 1982, Grazing impacts on Mars - A record of lost satellites In: *Lunar and Planetary Science Conference, 13th*, Houston, TX, March 15-19, 1982, Proceedings. Part 1. (A83-15326 04-91) Washington, DC, American Geophysical Union, 1982, p. A84-A96.
- Schultz, P.; Lutz, A. B., 1988, Polar wandering of Mars, *Icarus*, vol. 73, Jan. 1988, p. 91-141.
- Schultz, Peter H.; Wrobel, Kelly E., 2012, The oblique impact Hale and its consequences on Mars, *Journal of Geophysical Research*, Volume 117, Issue E4, CiteID E04001.
- Siegler, M. A.; Miller, R. S.; Keane, J. T.; Laneuville, M.; Paige, D. A.; Matsuyama, I.; Lawrence, D. J.; Crotts, A.; Poston, M. J., 2016, Lunar true polar wander inferred from polar hydrogen, *Nature*, Volume 531, Issue 7595, pp. 480-484
- Soto, A., Mischna, M., Schneider, T., Lee, C., Richardson, M., 2015, Martian atmospheric collapse: Idealized GCM studies, *Icarus*, 250, p. 553-569.
- Sprenke, Kenneth F., 2005, Martian magnetic paleopoles: A geostatistical approach, *Geophysical Research Letters*, Volume 32, Issue 9, CiteID L09201.
- Sprenke, Kenneth F.; Baker, Leslie L., 2000, Magnetization, Paleomagnetic Poles, and Polar Wander on Mars, *Icarus*, Volume 147, Issue 1, pp. 26-34.
- Sprenke, Kenneth F.; Baker, Leslie L.; Williams, Adele F., 2005, Polar wander on Mars: Evidence in the geoid, *Icarus*, Volume 174, Issue 2, p. 486-489.
- Stanley S, L Elkins-Tanton, MT Zuber, EM Parmentier, 2008, Mars' paleomagnetic field as the result of a single-hemisphere dynamo, *Science* 321 (5897), 1822-1825
- Steinberger, Bernhard; Torsvik, Trond H., 2008, Absolute plate motions and true polar wander in the absence of hotspot tracks, *Nature*, Volume 452, Issue 7187, pp. 620-623.

- Strom, Robert G.; Malhotra, Renu; Ito, Takashi; Yoshida, Fumi; Kring, David A., 2005, The Origin of Planetary Impactors in the Inner Solar System, *Science*, Volume 309, Issue 5742, pp. 1847-1850.
- Tanaka, K. L., S. J. Robbins, C. M. Fortezzo, J. A. Skinner, and T. M. Hare 2014. The digital global geologic map of Mars: Chronostratigraphic ages, topographic and crater morphologic characteristics, and updated resurfacing history. *Planetary and Space Science*, 95, p. 11-24.
- Touma, J. and Wisdom, J., 1993, The chaotic obliquity of Mars, *Science*, 259, p. 1294-1297.
- Tsai, Victor C.; Stevenson, David J., 2007, Theoretical constraints on true polar wander, *Journal of Geophysical Research: Solid Earth*, Volume 112, Issue B5, CiteID B05415.
- Walsh KJ, Morbidelli A, Raymond SN, O'Brien DP, Mandell AM. 2011. A low mass for Mars from Jupiter's early gas-driven migration. *Nature* 475:206–9.
- Weiss, D.K. and Head, J.W., 2015, Crater degradation in the Noachian highlands of Mars: Assessing the hypothesis of regional snow and ice deposits on a cold and icy early Mars, *Planetary and Space Science*, 117, p. 401-420.
- Wordsworth, Robin D., 2016, The Climate of Early Mars, *Annual Review of Earth and Planetary Sciences* 2016 44:1, 381-408.
- Zent, A., 2013, Orbital drivers of climate change on Earth and Mars, pp. 505-538 in *Comparative Climatology of the Terrestrial Planets*, edited by Stephen J. Mackwell et al., U. Arizona Press.
- Zhong, Shijie, 2009, Migration of Tharsis volcanism on Mars caused by differential rotation of the lithosphere, *Nature Geoscience*, Volume 2, Issue 1, pp. 19-23.
- Zuber, Maria T., 2007, Planetary science: Mars at the tipping point, *Nature*, Volume 447, Issue 7146, pp. 785-786.